Microporous phenol-formaldehyde resin-based adsorbents for pre-combustion CO_2 capture

C.F. Martín, M.G. Plaza, S. García, J.J. Pis, F. Rubiera, C. Pevida*

Instituto Nacional del Carbón (INCAR), CSIC. Apartado 73, 33080 Oviedo (Spain)

*corresponding author: *cpevida@incar.csic.es*

Abstract

Different types of phenolic resins were used as precursor materials to prepare adsorbents for the separation of CO_2 in pre-combustion processes. In order to obtain highly microporous carbons with suitable characteristics for the separation of CO_2 and H_2 under high pressure conditions, phenol-formaldehyde resins were synthesised under different conditions. Resol resins were obtained by using an alkaline environment while Novolac resins were synthesised in the presence of acid catalysts. In addition, two organic additives, ethylene glycol (E) and polyethylene glycol (PE) were included in the synthesis. The phenolic resins thus prepared were carbonised at different temperatures and then physically activated with CO_2. The carbons produced were characterised in terms of texture, chemical composition and surface chemistry. Maximum CO_2 adsorption capacities at atmospheric pressure were determined in a thermogravimetric analyser. Values of up to 10.8 wt.% were achieved. The high-pressure adsorption of CO_2 at room temperature was determined in a high-pressure magnetic suspension balance. The carbons tested showed enhanced CO_2 uptakes at high pressures (up to 44.7 wt.% at 25 bar). In addition, it was confirmed that capture capacities depend highly on the microporosity of the samples, the narrow micropores (pore widths of less than 0.7 nm) being the most active in CO_2 adsorption at atmospheric pressure. The results presented in this work suggest that phenol-formaldehyde resin-derived activated carbons, particularly those prepared with the addition of ethylene glycol, show great potential as adsorbents for pre-combustion CO_2 capture.

keywords: phenol-formaldehyde resin, CO_2 capture, adsorption.

1. Introduction

CO_2 is the main greenhouse gas that influences climate change, primarily via CO_2 emissions from the combustion of fossil fuels. Among the strategies considered to reduce CO_2 emissions to the atmosphere, carbon capture and storage (CCS) from large

point sources is the most promising alternative in the short to medium term. Adsorption is considered a very promising technology for CO_2 capture applications since the adsorbents have a high adsorption capacity, a great selectivity, good mechanical properties and they remain stable over repeated adsorption-desorption cycles [1,2]. Different types of solid sorbents have been, or are currently being, investigated as potential adsorbents for CO_2 capture. These include supported amines [3-5], carbon-based sorbents [6-12], supported carbonates [13] and zeolites [14-16]. The selective adsorption of CO_2 on inorganic and organic adsorbents like zeolite, silica gel, alumina and activated carbon is already used commercially for the separation of bulk CO_2 from gas mixtures and the removal of trace CO_2 from contaminated gases [17].

Activated carbons are also suitable candidates for CO_2 capture, their adsorption performance being dependent on the pore structure and the properties of the surface chemistry [18]. Although the capture capacities of activated carbons are, in general, lower than those of zeolites and molecular sieves under low pressure and ambient conditions, they offer the following advantages as CO_2 adsorbents: they have a large adsorption capacity at high pressure, they are easy to regenerate, they are cheap and not too sensitive to moisture. The use of naturally occurring precursors to produce activated carbons limits the purity, strength and physical form of the end-product materials. However, this drawback could be overcome by using polymeric precursors, where the reproducibility and purity of the precursor is within the control of the manufacturer and the physical forms and structures can be tailored by means of the polymer production process. Numerous polymer systems have been investigated as precursors of activated carbons. The cost of such materials is, however, implicitly linked to the cost of the polymer precursor and the carbon yield during the carbonisation and activation stages. Phenolic resins constitute a family of low-cost polymers, one of the most common being those produced from phenol and formaldehyde [19]. Phenolic resin-based activated carbons offer further advantages in that they can be produced in a wide variety of physical forms (e.g., granular or extruded, as fibres or as monolithic structures), they allow a close control of porosity, and they have a very low level of impurities and good physical strength [19-21].

In this work phenol-formaldehyde resins were employed as precursor materials for the preparation of microporous activated carbons for use in pre-combustion CO_2 capture

processes. This involves the removal of CO_2 from the shifted-syngas prior to the generation of electricity. As an alternative method for pre-combustion CO_2 capture, adsorption is considered a promising technology, as it offers potential energy savings compared to absorbent systems [22,23].

2. Experimental

2.1. Synthesis of Materials

Phenol-formaldehyde resins (from now on PFR) were used as precursor materials for the preparation of microporous carbon-based adsorbents. Depending on the formaldehyde-to-phenol ratio (F/P) and on the acid or basic nature of the catalyst, two methods were considered for the synthesis of PFR:

- The first one was basic catalysis using ammonium hydroxide (NH_4OH). This type of resin is commonly referred to as *Resol*. In this case a 1.5 formaldehyde-to-phenol ratio was used. This series will be denoted as PFN.
- The second one was acid catalysis with hydrochloric acid (HCl). In this case the formaldehyde-to-phenol ratio was around 1. These resins are called *Novolac*. This series will be denoted as PFCL.

In addition, four series of Novolac resins were prepared by incorporating two organic additives, ethylene glycol (E) and polyethylene glycol (PE), in two different proportions, 1 and 10 wt.%. These series will be referred to as E1, E10, PE1 and PE10, respectively. Table 1 summarises the conditions used in this work for the synthesis of phenol-formaldehyde resins. Phenol (99.4 %, BDH Prolabo) and formaldehyde (37 wt.% in H_2O, BDH Prolabo) were used to synthesize the resins. During the synthesis, the phenol-formaldehyde solution was mixed with the catalyst (acid or basic) in a flask equipped with a reflux condenser, stirred and heated up to the desired temperature. Once the synthesis had ended, the resins were cured, first in a rotary evaporator at 60-70 ºC under vacuum (absolute pressure 48-200 mbar) and then in a forced-air convection oven at 75-100 ºC for 24 h [24-28].

2.2. Carbonisation and physical activation with CO_2

The cured resins were carbonised and physically activated with CO_2 to generate microporosity in the samples. Carbonisation was performed in a horizontal furnace at temperatures up to 700-800 ºC (soaking time = 1 h) under a nitrogen flow rate of

50 mL min^{-1}. After this process the samples were activated in a vertical furnace in a 10 mL min^{-1} stream of CO_2 up to 750-900 ºC. Depending on the duration of the activation process, carbons with various degrees of burn off were obtained. Table 2 summarises the experimental conditions of the carbonisation and activation steps for the phenol-formaldehyde resin-based carbons prepared in this work.

2.3. Characterisation

The precursor materials and activated carbons were characterised in terms of thermal stability, chemical composition and texture:

- Thermal stability tests were carried out on the synthesised resins using a Setaram TGA 92 thermogravimetric analyser. The resins were heated up under an inert atmosphere (Ar, 50 mL min^{-1}) to 1000 ºC (heating rate, 15 ºC min^{-1}; soaking time, 30 min).
- The chemical characterisation involved proximate and ultimate analyses. In addition, the Point of Zero Charge (pH_{PZC}) was measured to obtain information about the acid or basic character of the resins. A mass titration method adapted from Noh and Schwarz was used for this purpose [29].
- For the textural characterisation, the surface areas and micropore volumes were evaluated from the N_2 and CO_2 adsorption isotherms at -196 ºC and 0 ºC, respectively. The isotherms were determined in a Micromeritics TriStar 3000 volumetric apparatus. The helium density was measured in an Accupyc 1330 at 35 ºC. Prior to any measurement, the samples were outgassed overnight at 100 ºC under vacuum.

  The surface areas were calculated by means of the BET equation and the micropore volumes were determined from the Dubinin-Radushkevich (DR) relation.

2.4. CO_2 Capture Capacity

The CO_2 adsorption potential of the samples at atmospheric pressure was assessed in a Setaram TGA 92 thermogravimetric analyser. In a typical experiment, around 20 mg of sample was loaded into the TGA and dried at 100 ºC under an inert atmosphere, prior to the adsorption experiment. Afterwards, a temperature-programmed CO_2 adsorption test was conducted at a very slow heating rate (0.5 ºC min^{-1}) from room temperature to 100 ºC. The maximum CO_2 uptake at atmospheric pressure was evaluated from the

increase in mass experienced by the samples when they were exposed to a pure stream of CO_2.

CO_2 adsorption isotherms were determined at 25 ºC up to 30 bar in a Rubotherm-VTI high-pressure magnetic suspension balance. First, the samples were outgassed at 100 ºC for 120 min under vacuum. Then, the system was cooled down to room temperature and sequentially pressurised (pressure steps ~ 2.5 bar) under a CO_2 atmosphere, from 0.2 to 30 bar, allowing the adsorption equilibrium to be reached.

3. Results and discussion

3.1. Thermal stability tests

Thermal degradation of phenol-formaldehyde resins mainly produces phenol and its methyl derivatives, as well as small amounts of simple aromatic hydrocarbons. Mechanisms to explain such degradation have been proposed in relation to the structure of phenol-formaldehyde resins [30]. *Novolacs* are made up of phenol units linked by methylene bridges whereas *Resols* also combine dimethylene ether groups (see Figures 1a and b). The incorporation of an organic additive during their synthesis introduces other types of ether cross-linking into the structure of the prepared resins (see Figure 1c). A high degree of cross-linking (i.e., in *Resols*) confers hardness, a good thermal stability and chemical imperviousness on the resins.

Although the proposed mechanisms seem to contradict each other, it can be concluded that a process of auto-oxidation of the methylene bridges during the thermal degradation of cured PFR takes place.

Figure 2 shows the TG and DTG curves obtained during the thermal stability tests of the phenol-formaldehyde resins synthesised in this work, i.e., PFN, PFCL, E1, E10, PE1 and PE10. According to the TG curves, PFN shows the highest thermal stability of the synthesised resins with a total mass loss of 40 wt.%. PFCL, E1 and PE1 show similar mass losses, around 50 wt.%. The addition of 10 wt.% ethylene and polyethylene glycol (E10 and PE10, respectively) results in an increase in mass loss of around 60 wt.%. In addition, E10 starts to decompose at a lower temperature. Analysis of the DTG curves points to the existence of three thermal degradation ranges: i) 100-300 ºC, ii) 300-470 ºC, and iii) 470-700 ºC. The first stage is controlled by the un-reacted groups, mainly methylol, which is present in the resin. It should be noted that E10 shows a

significant mass loss during this stage, suggesting the presence of free ethylene glycol (boiling point 196-198 ºC) in this resin. During the second stage, thermal degradation of the cross-linked network of the resin takes place. The formation of phenol and methyl derivatives, as well as the evolution of light gases (CH_4, CO, CO_2, etc.) may also occur. Un-reacted polyethylene glycol (boiling point around 400 ºC, according to tests carried out in our laboratory) may account for the important rate of mass loss of PE10 during this stage. PFN is the exception, as it mainly decomposes during the third stage. During this last stage, the degradation of the network continues, the C-H bond in phenol is broken and hydrogen gas evolves.

3.2. Chemical analysis

The proximate and ultimate analyses and the pH_{PZC} of the prepared carbons are presented in Table 3. The volatile matter content of the resin samples diminishes significantly during the activated carbon production process due to the devolatilisation of the functional labile groups through the effect of temperature. As a consequence, the hydrogen and oxygen contents also decrease. Carbon, which is more stable, increases in percentage with respect to the other elements. Activated resin-based samples with carbon contents > 96 wt.% are then produced.

After activation with CO_2, the pH increased and the activated samples became more basic than the initial resin sample. This effect was particularly significant in the resin series produced via acid catalysis. Basicity may have been due to oxygen coming from the activating gas (CO_2), that had been incorporated onto the surface of the char in the form of basic oxygen groups (i.e., pyrone) [31,32] or due to Lewis type basic sites associated to the carbon structure [33].

3.3. Textural characterisation

Figure 3 shows the N_2 and CO_2 adsorption isotherms of the phenol-formaldehyde resin-based activated carbons at -196 ºC and 0 ºC, respectively. Most of the phenol-formaldehyde resin-based activated carbons present nitrogen adsorption isotherms of type I, according to the BDDT classification [34], which is characteristic of microporous solids. The E10 and PE1 series show hysteresis loops at $p/p^0 > 0.4$ indicating the presence of a certain mesoporosity in these samples. For each series of activated carbons it can be seen that the higher the burn off degree of the activated

carbon, the greater the volume of nitrogen adsorbed. Carbon PFCLA9-42 showed the greatest N_2 uptake.

The CO_2 adsorption isotherms were used to assess the narrow microporosity (pore width < 1nm) in the samples. The shape of the isotherm indicates the micropore size distribution in the activated carbons. It can be observed that intensification of the activation treatment (higher burn-off degrees) results in CO_2 adsorption isotherms with more pronounced slopes that are characteristic of wider micropore size distributions. In contrast, lower burn-off degrees are characterised by CO_2 adsorption isotherms with pronounced elbows at low relative pressures that suggest narrower micropore size distributions. Carbon E1A8-42 showed the greatest CO_2 uptake.

Table 4 summarises the textural parameters, calculated from the N_2 and CO_2 adsorption isotherms and the helium density of the phenol-formaldehyde resin-based activated carbons.

The activated carbons showed helium densities of around 2 g cm^{-3}. Significant textural development, particularly in the microporosity domain, was achieved in the carbons activated to high burn off degrees. The PFCL and E1 series showed the greatest textural development, with BET surface areas (S_{BET}) of above 1300 m^2 g^{-1} and total micropore volumes ($W_{0,N2}$) of 0.5 cm^3 g^{-1}. Considering that lower temperatures of carbonisation and CO_2 activation were required to produce E1 activated carbons, the addition of 1 wt% ethylene glycol may have resulted in an enhancement of textural development.

The average micropore widths ($L_{0,N2}$), calculated from the Stoeckli-Ballerini relation [35], varied with the extent of activation (< 1 nm for the lower burn off and > 1 nm for the more activated samples). Narrow micropore volumes of between 0.2 and 0.3 cm^3 g^{-1} and an average narrow micropore width ($L_{0,CO2}$) of between 0.7 and 0.9 nm were achieved. The PE1 activated carbons showed a lower textural development compared to the other series. This may suggest differences in the effectiveness of polyethylene glycol and ethylene glycol as porogen agents.

From the results of textural characterisation, it can be concluded that activation with carbon dioxide develops texture in the phenol-formaldehyde resin-based activated carbons, particularly in the microporosity domain. In addition, larger degrees of burn-off not only increase the micropore volumes in the carbons but also widen microporosity.

3.4. Assessment of CO_2 capture capacity

Figure 4 shows the evolution of the mass of the samples with temperature, during the CO_2 capture tests conducted at atmospheric pressure in the TGA under a CO_2 flow rate of 50 mL min^{-1}. This mass gain was interpreted as the CO_2 uptake of the adsorbents and expressed in terms of mass of CO_2 per mass of dry adsorbent.

All the series of phenol-formaldehyde resin-based activated carbons presented a similar behaviour under these conditions: the capacity to adsorb CO_2 at atmospheric pressure diminished with the increase in temperature. This behaviour is typical of a physisorption based process. In addition, differences in capture capacity between carbons become shorter the higher the temperature. E1A75-16 showed the maximum CO_2 uptake at atmospheric pressure over the selected temperature range. PE1A9-36 lost its capacity to adsorb CO_2 at 85 ºC.

Figure 5a shows the maximum CO_2 capture capacities of the prepared phenol-formaldehyde resin-based activated carbons at atmospheric pressure and 25 ºC. Under these conditions, the maximum CO_2 uptake corresponded to E1A8-42 which reached 10.8 wt.%. The E1 series exhibited the best performance, with CO_2 uptakes of above 10 wt.%. The PFN and PFCL series reached capture capacities of around 9 wt.%. These values are in good agreement with those obtained for commercial activated carbons [10]. The poorest performance corresponded to the PE1 series which did not exceed 6 wt.%. It should be noted that for some carbon series (i.e., PFN or E1), intensification of the activation process did not enhance the capture capacity of the resultant activated carbon, whereas for others (i.e., PFCL or E10) it did.

Figure 5b shows the maximum CO_2 capture capacities of the prepared phenol-formaldehyde resin-based activated carbons at 25 bar and room temperature. As expected, capture capacities under these conditions were significantly higher than those at atmospheric pressure. Maximum CO_2 capture capacity also corresponded to E1A8-42 with an uptake of 44.7 wt.%. However, in this case, intensification of the activation process had a significant impact on the capture capacity of the activated carbons at 25 bar.

To relate the results of the CO_2 capture tests to the textural characteristics of the adsorbents, correlations between the CO_2 uptakes at 1 (Figure 6a) and 25 bar (Figure 6b) were correlated with the micropore volumes, $W_{0,N2}$ and $W_{0,CO2}$. The general trend

that can be observed in these figures is an increase in capture capacity with micropore volume. However, it can also be seen that activated carbons with similar micropore volumes show different capture capacities. This may be due to the different average micropore sizes.

Under atmospheric pressure, the capacity to adsorb CO_2 appears to correlate better with narrow microporosity ($W_{0,CO2}$). Previous studies have shown that only pore sizes less than 5 times that of the molecular size of the adsorbate are effective for gas adsorption at atmospheric pressure. In the particular case of CO_2, it has been demonstrated empirically [36] as well as by mathematical simulation, using grand canonical Monte Carlo (GCMC) and the nonlocal density functional theory (NLDFT) [37], that only pores of less than 1 nm can be effective for CO_2 adsorption at atmospheric pressure. In contrast, at 25 bar, it is the total microporosity ($W_{0,N2}$) in the phenol-formaldehyde resin-derived activated carbons that seems to determine the CO_2 capture capacity. At high pressures CO_2 is also adsorbed in the super-microporosity range (pore sizes between 0.7 and 2 nm) [38].

In a previous work, we demonstrated that from these correlations it is possible to estimate the theoretical limits of the CO_2 capture capacity of an activated carbon under atmospheric and high pressures [39].

4. Conclusions

Activation with carbon dioxide develops the texture of phenol-formaldehyde resin-based activated carbons, particularly in the microporosity domain. Larger burn-off degrees not only increase micropore volume in carbons but also widen microporosity. The addition of ethylene glycol up to 1 wt% results in an enhancement of the textural development due to the lower temperatures of carbonisation and activation with CO_2.

Even though the chemical and textural characteristics of the resin carbons were similar, significant differences in their CO_2 capture performance were observed. E1 activated carbons displayed the greatest uptakes at room temperature and atmospheric pressure (1 bar), with CO_2 capture capacities of above 10 wt.%. At high pressure (25 bar) and room temperature the CO_2 uptakes of the phenol-formaldehyde resin-based activated carbons varied considerably depending on the degree of activation. The greatest uptake, 44.7 wt.%, was achieved by the E1 carbon activated to 42 % burn off.

It has been demonstrated that under atmospheric pressure, the capacity to adsorb CO_2 appears to correlate better with narrow microporosity ($W_{0,CO2}$), whereas at 25 bar, it is the total microporosity ($W_{0,N2}$) of phenol-formaldehyde resin-derived activated carbons that seems to determine CO_2 capture capacity.

From the results presented it can be concluded that phenol-formaldehyde resin carbons, particularly those prepared with the addition of 1 wt% of ethylene glycol, show promising characteristics for application in pre-combustion CO_2 capture processes. Further research is currently being undertaken in our research group to tailor and improve the characteristics of resin-based adsorbents without increasing the cost of the production process.

Acknowledgements

This work was carried out with financial support from the Spanish MICINN (Project ENE2008-05087). C.F.M. acknowledges support from the CSIC JAE-Predoc Program co-financed by the European Social Fund.

Table 1 Experimental conditions used in the synthesis of phenol-formaldehyde resins

Resins	F/P	Additive	Catalyst (mL)	T (ºC)	Time (h)
PFN	1.5	–	14 – NH_4OH (28 wt.%)	80	1
PFCL	0.98	–	2 – HCl (37 wt%)	95	0.75
E1	1	2.6 mL	2 – HCl (37 wt%)	95	1.5
E10	1	29 mL	2 – HCl (37 wt%)	95	2.8
PE1	1.04	1 g	2 – HCl (37 wt%)	95	0.75
PE10	1.02	10.9 g	2 – HCl (37 wt%)	95	1

Table 2 Experimental conditions of the carbonisation and activation steps of the phenol-formaldehyde resin-based activated carbons

Sample	Carbonisation		CO_2 activation	
	T (ºC)	yield (%)*	T (ºC)	burn-off (%)
PFNA9-20	800	42	900	20
PFNA9-38	800	42	900	38
PFCLA9-20	800	51	900	20
PFCLA9-42	800	51	900	42
E1A75-16	700	55	750	16
E1A8-24	700	55	800	24
E1A8-42	700	55	800	42
E10A9-22	800	61	900	22
E10A9-46	800	61	900	46
PE1A9-20	800	50	900	20
PE1A9-28	800	50	900	28
PE1A9-36	800	50	900	36

* *yield (%) =* $(m_i\text{-}m_f)\ 100 / m_i$, where m_i is the mass of cured resin and m_f is the mass of char produced after carbonisation

Note: PE10 was not activated with CO_2 *due to the lack of mechanical strength of the char.*

Table 3 Chemical characteristics of the synthesised phenol-formaldehyde resins and derived activated carbons

Sample	Proximate Analysis (wt.%, db)	Ultimate Analysis (wt.%, db)				pH_{PZC}
	VM	C	H	N	O*	
PFN series						
PFN	41.3	72.7	6.6	4.5	16.2	8.3
PFNA9-20	2.0	96.3	0.1	0.9	2.7	8.9
PFNA9-38	4.1	97.3	0.3	0.9	1.5	8.8
PFCL series						
PFCL	41.2	82.6	6.0	–	11.4	5.2
PFCLA9-20	1.1	96.7	0.1	–	3.2	8.6
PFCLA9-42	2.3	97.4	0.1	–	2.5	9.4
E1 series						
E1	40.9	80.8	5.9	–	13.3	4.5
E1A75-16	3.3	96.8	0.3	–	2.9	8.6
E1A8-24	3.4	97.0	0.2	–	2.8	8.9
E1A8-42	2.8	97.2	0.1	–	2.7	8.8
E10 series						
E10	43.8	77.8	6.2	–	16.0	4.3
E10A9-22	1.3	97.3	0.1	–	2.6	8.5
E10A9-46	1.4	96.3	0.1	–	3.6	9.1
PE1 series						
PE1	40.0	81.1	5.9	–	13.0	4.5
PE1A9-20	2.3	97.4	0.1	–	2.5	8.5
PE1A9-28	3.0	97.0	0.2	–	2.8	8.6
PE1A9-36	1.8	97.2	0.1	–	2.7	7.5
*PE10 series***						
PE10	31.3	75.8	6.4	–	17.8	4.5

VM: volatile matter; db: dry basis; *: calculated by difference; ** PE10 was not activated with CO_2 due to the lack of mechanical strength of the char.

Table 4 Textural parameters calculated from the N_2 and CO_2 adsorption isotherms of the phenol-formaldehyde resin-based activated carbons

Sample	d_{He} (g cm^{-3})	N_2 ads. at -196ºC				CO_2 ads. at 0ºC	
		S_{BET} (m^2 g^{-1})	V_p (cm^3 g^{-1})	$W_{0,N2}$ (cm^3 g^{-1})	$L_{0,N2}$ (nm)	$W_{0,CO2}$ (cm^3 g^{-1})	$L_{0,CO2}$ (nm)
PFN series							
PFNA9-20	2.02	755	0.31	0.29	0.84	0.29	0.68
PFNA9-38	2.08	1211	0.52	0.45	1.26	0.26	0.70
PFCL series							
PFCLA9-20	1.95	626	0.27	0.24	0.96	0.22	0.71
PFCLA9-42	2.11	1381	0.62	0.51	1.45	0.29	0.74
E1 series							
E1A75-16	1.85	781	0.31	0.31	0.85	0.32	0.66
E1A8-24	1.85	841	0.37	0.33	0.90	0.33	0.69
E1A8-42	1.96	1369	0.60	0.51	1.15	0.33	0.73
E10 series							
E10A9-22	1.89	538	0.27	0.21	1.04	0.23	0.73
E10A9-46	2.06	1103	0.58	0.40	1.38	0.33	0.87
PE1 series							
PE1A9-20	1.81	306	0.20	0.12	1.07	0.15	0.71
PE1A9-28	1.90	553	0.33	0.22	1.12	0.20	0.70
PE1A9-36	2.03	790	0.40	0.30	1.31	0.26	0.73

Figure 1

a)

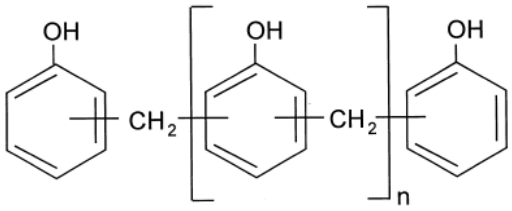

b)

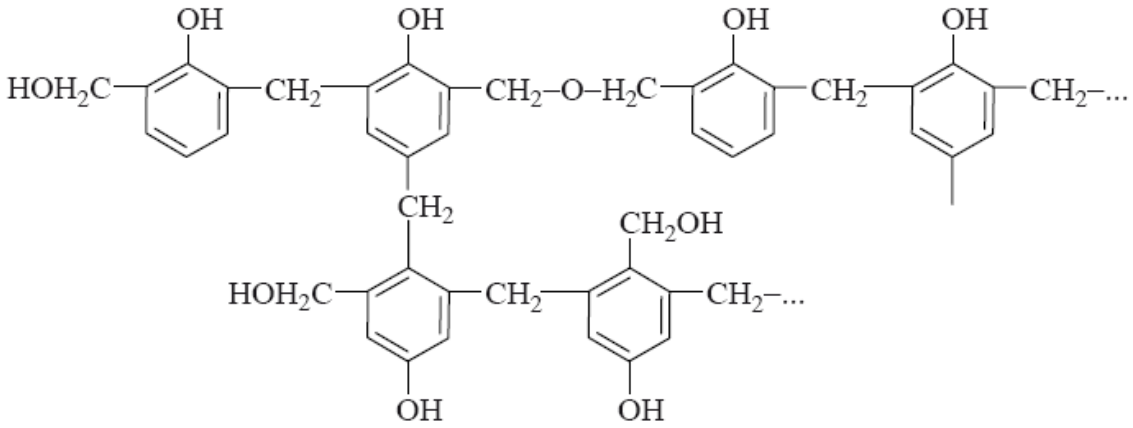

c)

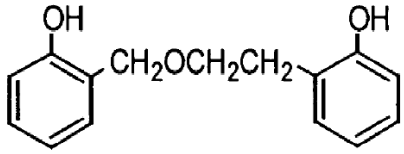

Figure 1. Structure of phenol-formaldehyde resins: a) Novolac, b) Resol, and c) Novolac with addition of ethylene glycol.

Figure 2

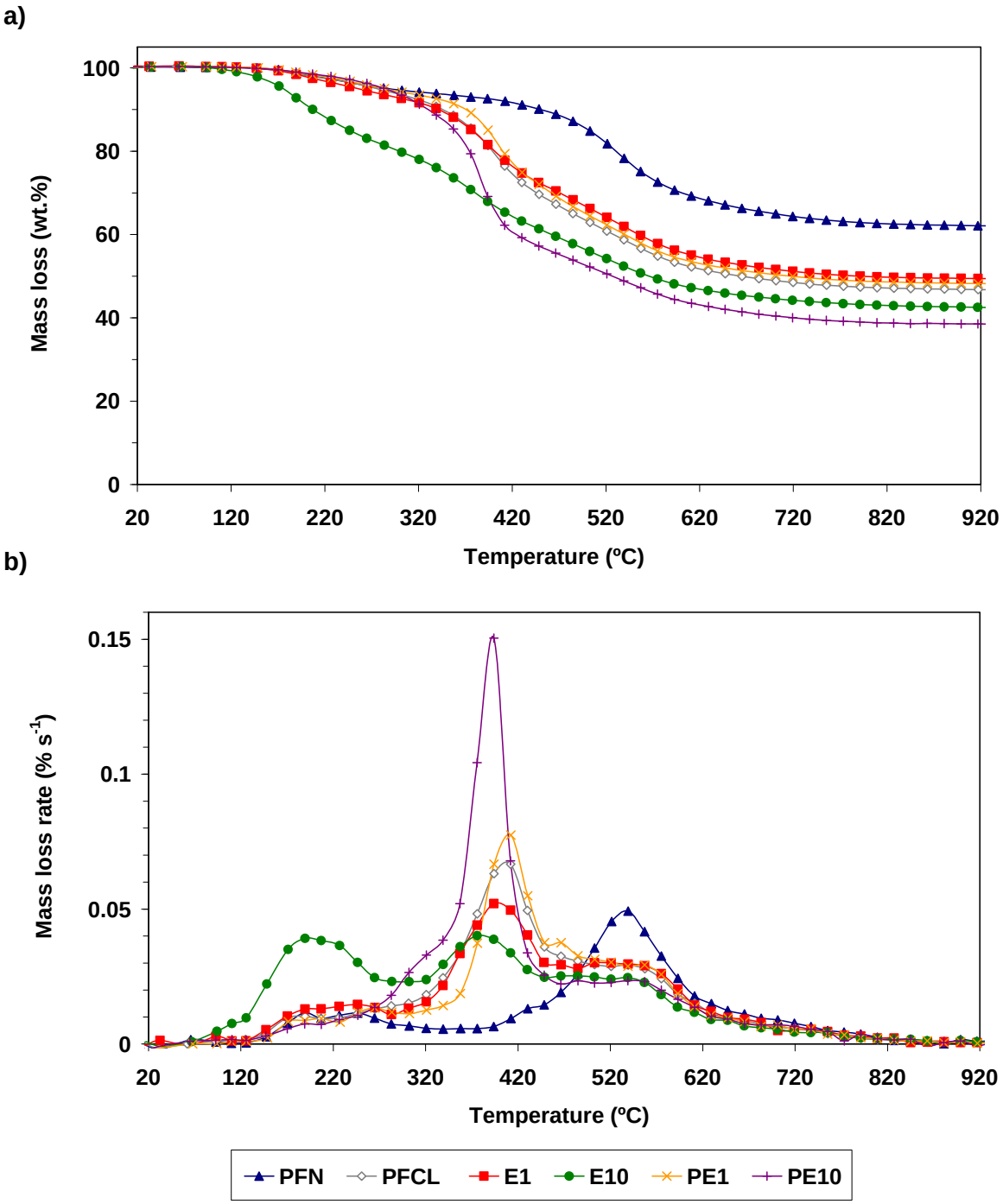

Figure 2. Thermal stability tests of the phenol-formaldehyde resins a) TG curves, and b) DTG curves.

Figure 3

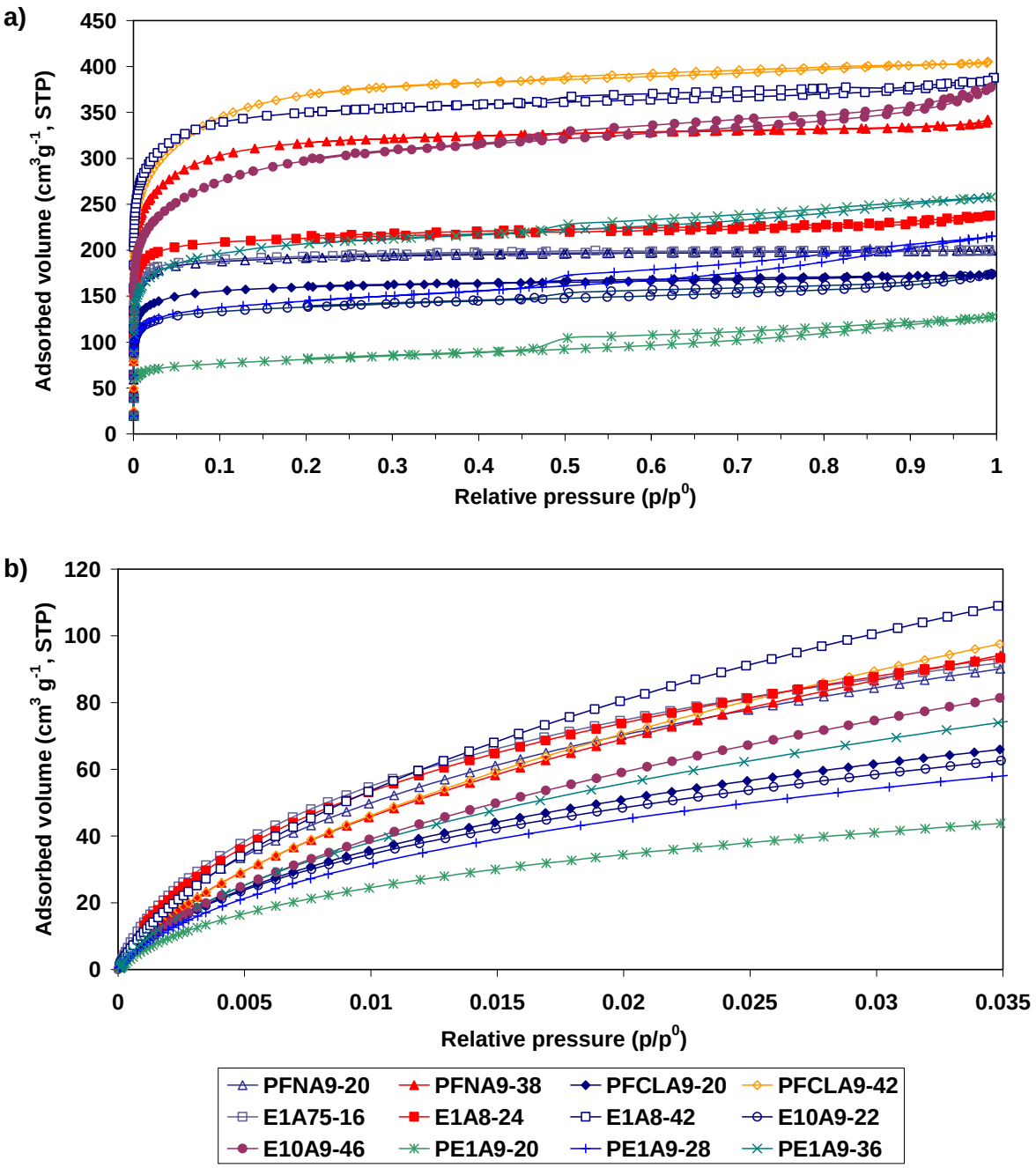

Figure 3. Adsorption isotherms of the phenol-formaldehyde resin-based activated carbons a) N_2 at -196 ºC, and b) CO_2 at 0 ºC.

Figure 4

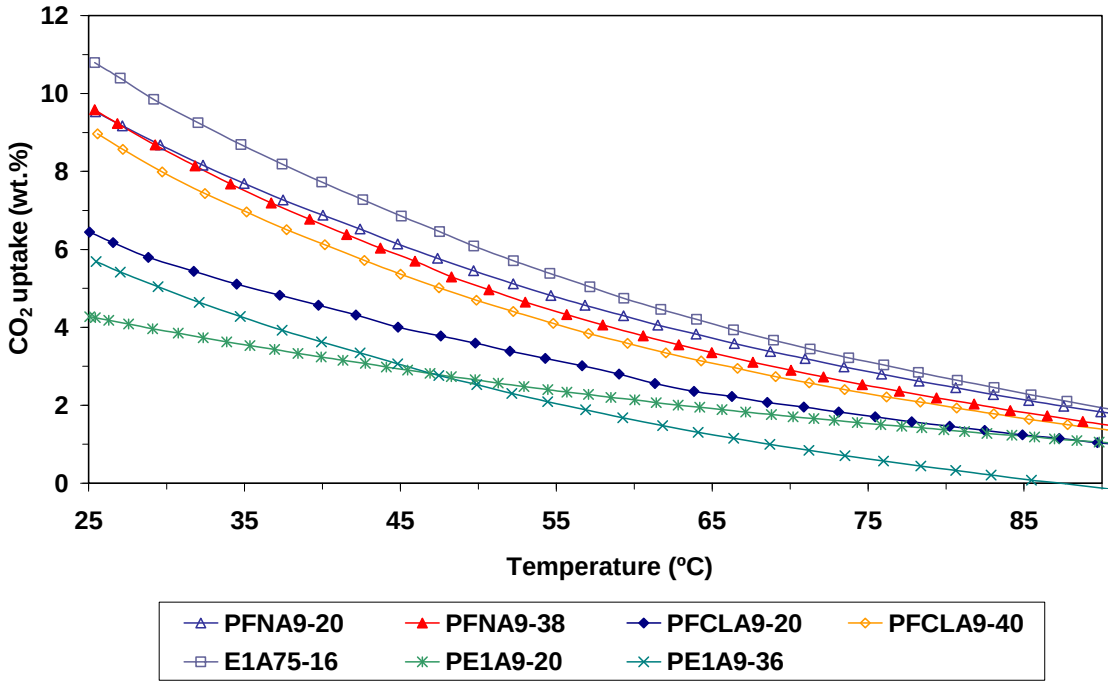

Figure 4. CO_2 capture capacity profile of phenol-formaldehyde resin-based activated carbons, at atmospheric pressure, in the 25-90 ºC temperature range.

Figure 5

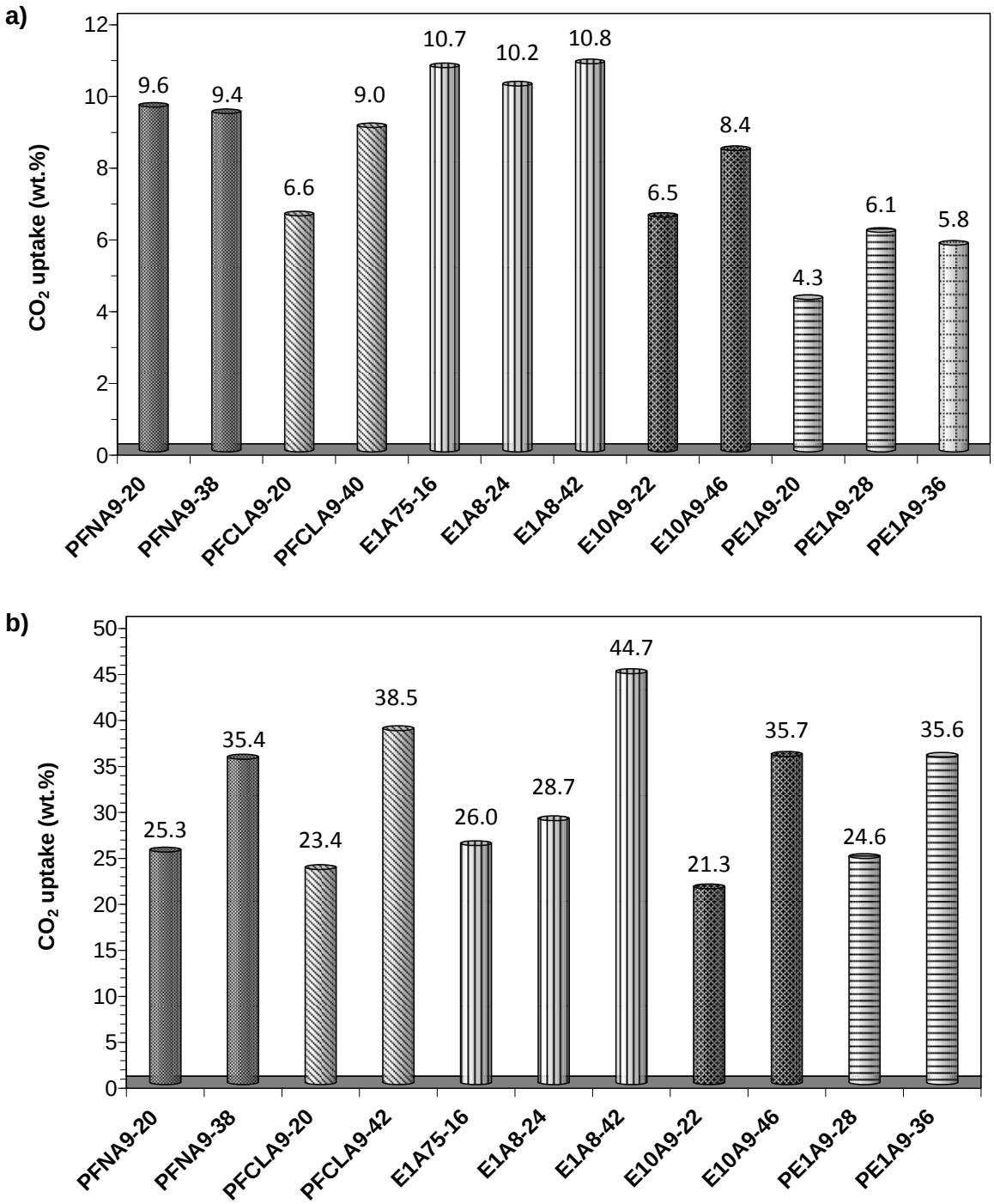

Figure 5. Maximum CO_2 capture capacities of the phenol-formaldehyde resin-based activated carbons, a) at atmospheric pressure and room temperature and b) at 25 bar and room temperature.

Figure 6

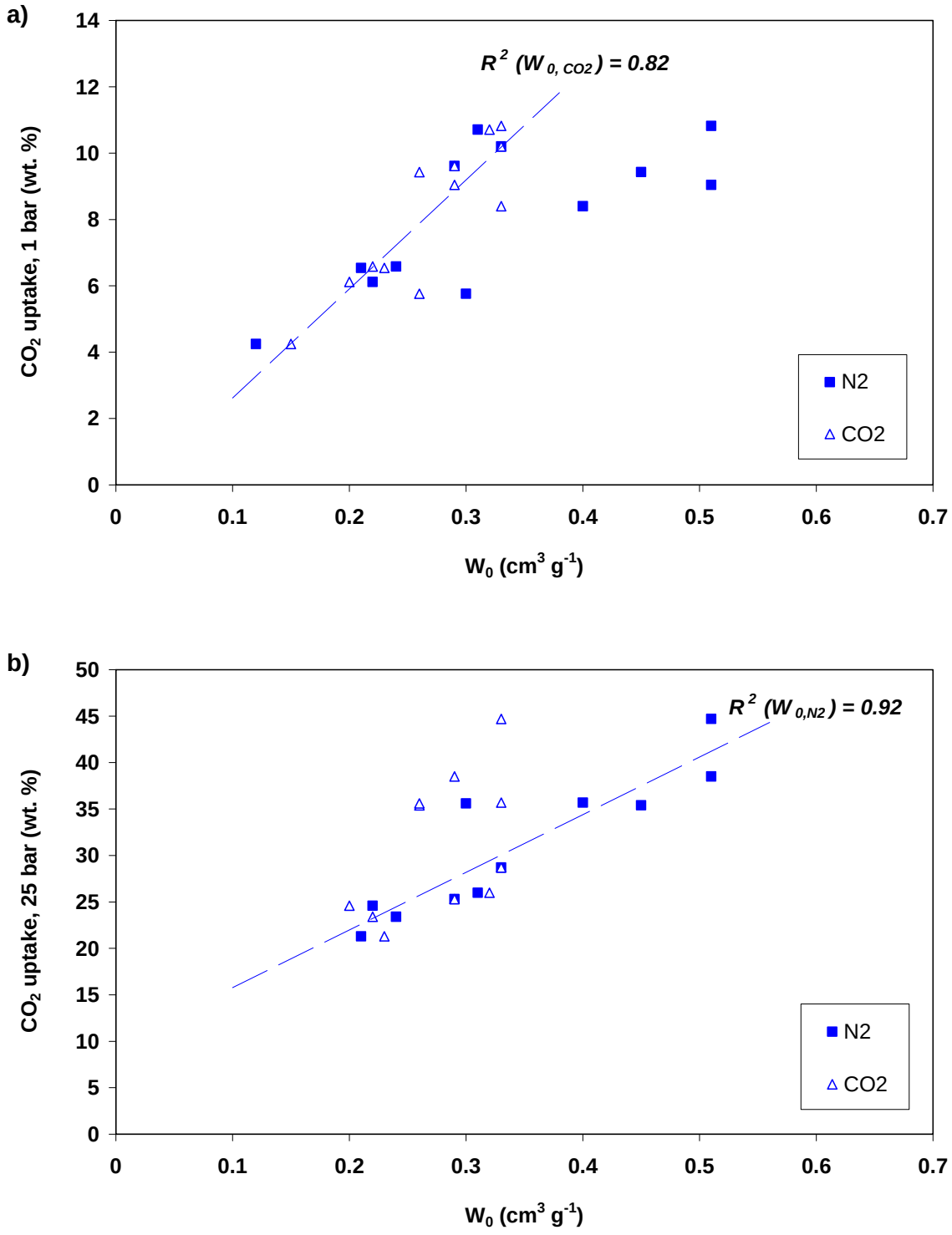

Figure 6. Correlation of the CO_2 uptakes with micropore volumes, $W_{0,N2}$ and $W_{0,CO2}$, a) at room temperature and atmospheric pressure and b) at 25 bar and room temperature.

.4. References

[1] Yong Z., Mata V., Rodrigues A.E. Adsorption of carbon dioxide at high temperature—a review. Separation and Purification Technology 2002; 26: 195-203

[2] Choi S., Drese J.H., Jones C.W. Adsorbent materials for carbon dioxide capture from large anthropogenic point sources. ChemSusChem 2009; 2: 796-854

[3] Knowles G.P., Delaney S.W., Chaffee A.L. Diethylenetriamine[propyl(silyl)]-functionalized (DT) mesoporous silicas as CO_2 adsorbents. Industrial and Engineering Chemistry Research 2006; 45: 2626-33

[4] Gray M.L., Soong Y., Champagne K.J., Baltrus J., Stevens Jr R.W., Toochinda P., Chuang S.S.C. CO_2 capture by amine-enriched fly ash carbon sorbents. Separation and Purification Technology 2004; 35: 31-6

[5] Plaza M.G., Pevida C., Arias B., Fermoso J., Arenillas A., Rubiera F., Pis J.J. Application of thermogravimetric analysis to the evaluation of aminated solid sorbents for CO_2 capture. Journal of Thermal Analysis and Calorimetry 2008; 92: 601-6

[6] Maroto-Valer M.M., Tang Z., Zhang Y. CO_2 capture by activated and impregnated anthracites. Fuel Processing Technology 2005; 86: 1487-502

[7] Plaza M.G., Pevida C., Arenillas A., Rubiera F., Pis J.J. CO_2 capture by adsorption with nitrogen enriched carbons. Fuel 2007; 86: 2204-12

[8] Plaza M.G., Pevida C., Arias B., Fermoso J., Rubiera F., Pis J.J. A comparison of two methods for producing CO_2 capture adsorbents. Energy Procedia 2009; 1: 1107-13

[9] Plaza M.G., Pevida C., Arias B., Fermoso J., Casal M.D., Martín C.F., Rubiera F., Pis J.J. Development of low-cost biomass-based adsorbents for postcombustion CO_2 capture. Fuel 2009; 88: 2442-7

[10] Pevida C., Plaza M.G., Arias B., Fermoso J., Rubiera F., Pis J.J. Surface modification of activated carbons for CO_2 capture. Applied Surface Science 2008; 254: 7165-72

[11] Pevida C., Snape C.E., Drage T.C. Templated polymeric materials as adsorbents for the postcombustion capture of CO_2. Energy Procedia 2009; 1: 869-74

[12] Drage T.C., Blackman J.M., Pevida C., Snape C.E. Evaluation of activated carbon adsorbents for CO_2 capture in gasification. Energy & Fuels 2009; 23: 2790-6

[13] Shigemoto N., Yanagihara T., Sugiyama S., Hayashi H. Material balance and energy consumption for CO_2 recovery from moist flue gas employing K_2CO_3-on-activated carbon and its evaluation for practical adaptation. Energy & Fuels 2006; 20: 721-6

[14] Merel J., Clausse M., Meunier F. Experimental investigation on CO_2 post-combustion capture by indirect thermal swing adsorption using 13X and 5A zeolites. Industrial and Engineering Chemistry Research 2008; 47: 209-15

[15] Ko D., Siriwardane R., Biegler L.T. Optimization of a pressure-swing adsorption process using zeolite 13X for CO_2 sequestration. Industrial and Engineering Chemistry Research 2003; 42: 339-48

[16] Cavenati S., Grande C.A., Rodrigues A.E. Adsorption equilibrium of methane, carbon dioxide, and nitrogen on zeolite 13X at high pressures. Journal of Chemical and Engineering Data 2004; 49: 1095-101

[17] Ruthven D.M. In: Principles of adsorption and adsorption processes. John Wiley & Sons. New York, 1984,

[18] Sircar S., Golden T.C., Rao M.B. Activated carbon for gas separation and storage. Carbon 1996; 34: 1-12

[19] Knop A., Pilato L.A. In: Phenolic Resins. Chemistry, Applications and Performance. Springer-Verlag. Berlin, 1985,

[20] Foster A.I., Linney H.J., Tennison S.R., Cory R.A., Swan D.P. The use of carbons produced from phenolic resins for flue gas desulphurization. Fuel 1993; 72: 337-42

[21] Tennison S.R. Phenolic-resin-derived activated carbons. Applied Catalysis A: General 1998; 173: 289-311

[22] Yang R.T. In: Gas separation by adsorption processes. Imperial College Press. 1997,

[23] Ruthven D.M., Farooq S., Knaebel K.S. In: Pressure Swing Adsorption. John Wiley & Sons, Inc. 1994,

[24] Lin C.-C. , Teng H. Influence of the formaldehyde-to-phenol ratio in resin synthesis on the production of activated carbons from phenol-formaldehyde resins. Industrial and Engineering Chemistry Research 2002; 41: 1986-92

[25] Horikawa T., Ogawa K., Mizuno K., Hayashi J., Muroyama K. Preparation and characterization of the carbonized material of phenol–formaldehyde resin with addition of various organic substances. Carbon 2003; 41: 465-72
[26] Teng H., Wang S.-C. Influence of oxidation on the preparation of porous carbons from phenol-formaldehyde resins with KOH activation. Industrial and Engineering Chemistry Research 2000; 39: 673-8
[27] Teng H., Wang S.-C. Preparation of porous carbons from phenol-formaldehyde resins with chemical and physical activation. Carbon 2000; 38: 817-24
[28] Shafizadeh J.E., Guionnet S., Tillman M.S., Seferis J.C. Synthesis and characterization of phenolic resole resins for composite applications. Journal of Applied Polymer Science 1999; 73: 505-14
[29] Noh J.S., Schwarz J.A. Estimation of the point of zero charge of simple oxides by mass titration. Journal of Colloid and Interface Science 1989; 130: 157-64
[30] Chen Y., Chen Z., Xiao S., Liu H. A novel thermal degradation mechanism of phenol-formaldehyde type resins. Thermochimica Acta 2008; 476: 39-43
[31] Huang M.-C., Teng H. Urea impregnation to enhance porosity development of carbons prepared from phenol–formaldehyde resins. Carbon 2002; 40: 955-71
[32] Papirer E., Li S., Donnet J.-B. Contribution to the study of basic surface groups on carbons. Carbon 1987; 25: 243-7
[33] Leon y Leon C.A., Solar J.M., Calemma V., Radovic L.R. Evidence for the protonation of basal plane sites on carbon. Carbon 1992; 30: 797-811
[34] Brunauer S., Deming L.S., Deming W.E., Teller E. On a theory of the van der Waals adsorption of gases. Journal of the American Chemical Society 1940; 62: 1723-32
[35] Stoeckli F., Ballerini L. Evolution of microporosity during activation of carbon. Fuel 1991; 70: 557-9
[36] Martin-Martinez J.M., Torregrosa-Macia R., Mittelmeijer-Hazeleger M.C. Mechanisms of adsorption of CO_2 in the micropores of activated anthracite. Fuel 1995; 74: 111-4
[37] Vishnyakov A., Ravikovitch P.I., Neimark A.V. Molecular level models for CO_2 sorption in nanopores. Langmuir 1999; 15: 8736-42
[38] Cazorla-Amoros D., Alcaniz-Monge J., Linares-Solano A. Characterization of activated carbon fibers by CO_2 adsorption. Langmuir 1996; 12: 2820-4
[39] Martín C.F., Plaza M.G., Pis J.J., Rubiera F., Pevida C., Centeno T.A. On the limits of CO_2 capture capacity of carbons. Separation and Purification Technology 2010; 74: 225-9